RSC Advances

PAPER

View Article Online
View Journal | View Issue

Cite this: *RSC Adv.*, 2018, **8**, 12870

Characterization of CMC–LDH beads and their application in the removal of Cr(VI) from aqueous solution

Li Tan, Hailong Li and Mengru Liu*

Received 22nd January 2018
Accepted 20th March 2018

DOI: 10.1039/c8ra00633d

rsc.li/rsc-advances

In this study, CMC–LDH beads were prepared and characterized using SEM, FTIR and TG analysis. The beads were applied for the removal of Cr(VI) from aqueous solution. The effects of adsorbent dosage, initial pH and initial concentration of Cr(VI) solution on Cr(VI) uptake were investigated in detail. Moreover, adsorption isotherms and adsorption kinetic models were employed to analyze the adsorption process, and a preliminary study of the reusability of the adsorbent was performed. The experimental results showed that the CMC–LDH beads could remove Cr(VI) from aqueous solution efficiently. When the initial concentration of the Cr(VI) solution was 100 mg L^{-1} and the adsorbent dosage was 12 g L^{-1}, the removal efficiency of Cr(VI) reached 96.2%. After the CMC–LDH beads were reused 10 times, the removal efficiency of Cr(VI) still remained at 89.6%.

1. Introduction

Heavy metal pollution has attracted widespread attention due to the high toxicity and irreversibility, which could cause environmental pollution even at low levels. Chromium is a toxic heavy metal which can easily contaminate soil and water and can harm people's health. Due to its wide industrial use, chromium pollution most commonly arises from mining, electroplating, leather making, *etc.* Chromium mainly exists in hexavalent [CrO_4^{2-}, $Cr_2O_7^{2-}$ and Cr(VI)] and trivalent [$Cr(OH)_3$ and Cr(III)] forms in the natural environment. Cr(VI) is a naturally occurring metal, the ratio of hexavalent chromium to total chromium is less than 3%. However, chromium has the characteristics of high toxicity and high solubility and is carcinogenic, which could lead to hepatic or renal damage, gastrointestinal irritation, central nervous system irritation,[1,2] *etc.* It has been reported that Cr(VI) is much more toxic than Cr(III).[3] In China, chromium salt induction is one of the most serious pollution, and the removal or disposal of heavy metal pollutants from wastewater is an urgent problem to be solved. Different technologies[4] for the removal of heavy metal ions, including chemical precipitation, ion-exchange, adsorption, membrane filtration and electrochemical treatment, have been used. Among them, the adsorption process is recognized as an effective and economical method for wastewater treatment, and the application of low-cost adsorbents for wastewater treatment is an area of great interest for scientific researchers.

Carboxymethylcellulose (CMC), a derivative of natural cellulose produced *via* alkalization and etherification, is abundant, reproducible and biodegradable.[5,6] CMC contains a large number of hydroxyl groups and carboxyl groups in its molecular chain, both of which can react with metal ions. Layered double hydroxides (LDHs) are layered materials with a chemical composition represented by the general formula $[M(II)_{1-x}\text{-}M(III)_x(OH)_2]^{x+}[A_{x/n}{}^{n-}]\cdot mH_2O$,[7] where M(II) and M(III) are divalent and trivalent metal ions, respectively; A^{n-} represents charge compensation anions or gallery anions, such as CO_3^{2-}, Cl^-, or organic anions; x is the ratio of M(III) to the total amount of M(II) and M(III), and m represents the amount of crystallization water.[8,9] Due to their special layered structure, low cost and ease of synthesis, LDHs can be used as adsorbents to treat heavy metal ions in contaminated water,[10,11] and they exhibit good application prospects for environmental pollution control.

CMC is transparent, non-toxic, biocompatible and biodegradable. LDHs have unique characteristics, such as their facile synthesis, versatility and tunable composition, which make them attractive for the preparation of bio-nanocomposites. In the presence of Al^{3+} or Fe^{3+}, a mixture of CMC and LDHs can result in the formation of uniform and small-sized spherical beads. In recent years, some research has focused on the preparation of CMC–LDH composite materials and their application in the medical field,[12,13] whereas their application for wastewater treatment has rarely been reported in the literature. Considering the factors mentioned above, a coprecipitation method was employed for the preparation of LDHs in this study. Then we attempted to prepare a kind of spherical adsorbent, which is expected to be more convenient to use and recycle than pure LDHs for the adsorption of heavy metal ions. The synthesized products were characterized using scanning electron microscopy (SEM), Fourier transform infrared spectroscopy (FTIR) and thermogravimetric (TG) analysis. Furthermore, the resulting CMC–LDH beads were used for the removal of Cr(VI) from aqueous solution. The impact of various factors, such as adsorbent

State Key Laboratory of Pulp and Paper Engineering, South China University of Technology, Guangzhou 510640, China. E-mail: lmr@scut.edu.cn

dosage, pH and contact time, on the removal rate of Cr(VI) during the adsorption process was investigated. Moreover, adsorption isotherms and adsorption kinetic models were employed to analyze the adsorption behavior. Finally, a preliminary study of the reusability of the adsorbent was performed.

2. Experimental section

2.1 Materials

CMC, with a degree of substitution (DS) of 0.7 and a viscosity of 50–100 mPa s (1% in H_2O, 25 °C), was purchased from Aladdin Chemistry Co. Ltd, China. All of the other chemicals used in the present research were of analytical grade and were obtained from Guangzhou Chemical Reagent Factory, China.

2.2 Preparation of LDHs

Mg–Al–LDH was prepared *via* a coprecipitation method.[14] Firstly, a nitrate solution was prepared by dissolving 0.12 mol $Mg(NO_3)_2 \cdot 6H_2O$ and 0.04 mol $Al(NO_3)_3 \cdot 9H_2O$ in distilled water. Then the resulting aqueous solution was made up to 100 mL. Meanwhile, an alkaline solution was made up to 160 mL with 0.32 mol NaOH and 0.08 mol $NaNO_3$. Secondly, the alkaline solution was added dropwise to the metal nitrate solution over 2 hours (2 h) under a N_2 atmosphere. The pH of the slurry was adjusted to 10 using NaOH solution, and the slurry was crystallized at 70 °C for 24 h. Afterwards, the precipitate was centrifuged and washed with distilled water to neutralise the LDH and it was then dried at 50 °C.

2.3 Preparation of CMC–LDH beads

4 g LDH was dispersed in 100 mL distilled water. Then, 2 g CMC was added into this solution with continuous stirring until a homogeneous solution was obtained. Afterwards, the homogeneous solution was added drop-wise into a 100 mL Al^{3+} solution (0.1 mol L^{-1}) using a syringe. After that, the beads were crosslinked with Al^{3+} for 2 h. Finally, the resulting CMC–LDH beads were rinsed with deionized water to remove unreacted Al^{3+} and they were then dried at 50 °C.

2.4 Characterization

Infrared spectra were obtained using a FTIR spectrometer (Bruker Instruments, model VerTex70, Germany) in the 4000–400 cm^{-1} range at a resolution of 0.5 cm^{-1} with KBr pellets. Scanning electron microscopy (SEM) images were obtained using a scanning electronic microscope (Zeiss Instruments, model Merlin, Germany) operating at 5 kV. The thermal properties were measured using a simultaneous thermal analyzer (NETZSCH, model STA449 F3, Germany), and 10 mg samples were heated from room temperature to 600 °C at a heating rate of 10 °C min^{-1} under a N_2 atmosphere.

2.5 Adsorption experiment

A stock solution of Cr(VI) was prepared using potassium dichromate, which was dried at 120 °C for 2 h in advance. All of the adsorption experiments were conducted in 250 mL beaker flasks containing 100 mL Cr(VI) solution, which were equilibrated at 180 rpm. The effect of initial pH (varied from 3 to 8) and adsorbent dosage (varied from 4 to 16 g L^{-1}) on the removal of Cr(VI) using CMC–LDH beads was investigated, with an initial concentration of 100 mg L^{-1} at 35 °C. The impact of contact time was also investigated, with an initial concentration of 100 mg L^{-1} at 35 °C. During the kinetic adsorption experiments, samples were collected after 5, 10, 15, 20, 30, 40, 60, 80, 100, 120, 150 and 180 min of agitation. In addition, the adsorption isotherm experiments were conducted in the range 20–40 °C with various initial concentrations of Cr(VI), ranging from 100 to 500 mg L^{-1}.

The adsorption capacity and removal rate of Cr(VI) were calculated using the following equations:

Adsorption capacity:

$$q_e = \frac{C_0 - C_e}{W} V \quad (1)$$

Removal rate:

$$R = \frac{C_0 - C_t}{C_0} \quad (2)$$

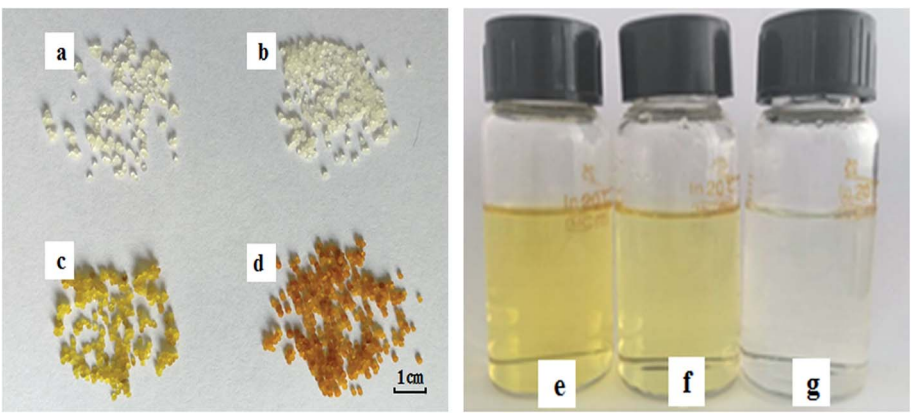

Fig. 1 Digital photographs of the CMC beads (a), CMC–LDH beads (b), CMC beads after adsorbing Cr(VI) (c), CMC–LDH beads after adsorbing Cr(VI) (d), Cr(VI) solution with a concentration of 100 mg L^{-1} (e) and Cr(VI) solution with a concentration of 100 mg L^{-1} after adsorption by the CMC beads (f) and CMC–LDH beads (g).

where C_0 and C_e represent the initial and equilibrium concentrations of Cr(VI) (mg L^{-1}), respectively, V is the volume of the Cr(VI) solution and W is the weight of the dried adsorbent.

2.6 Desorption experiment

In this study, desorption experiments were conducted using 1 mol L^{-1} $NaNO_3$ solution. The adsorbed saturated CMC–LDH

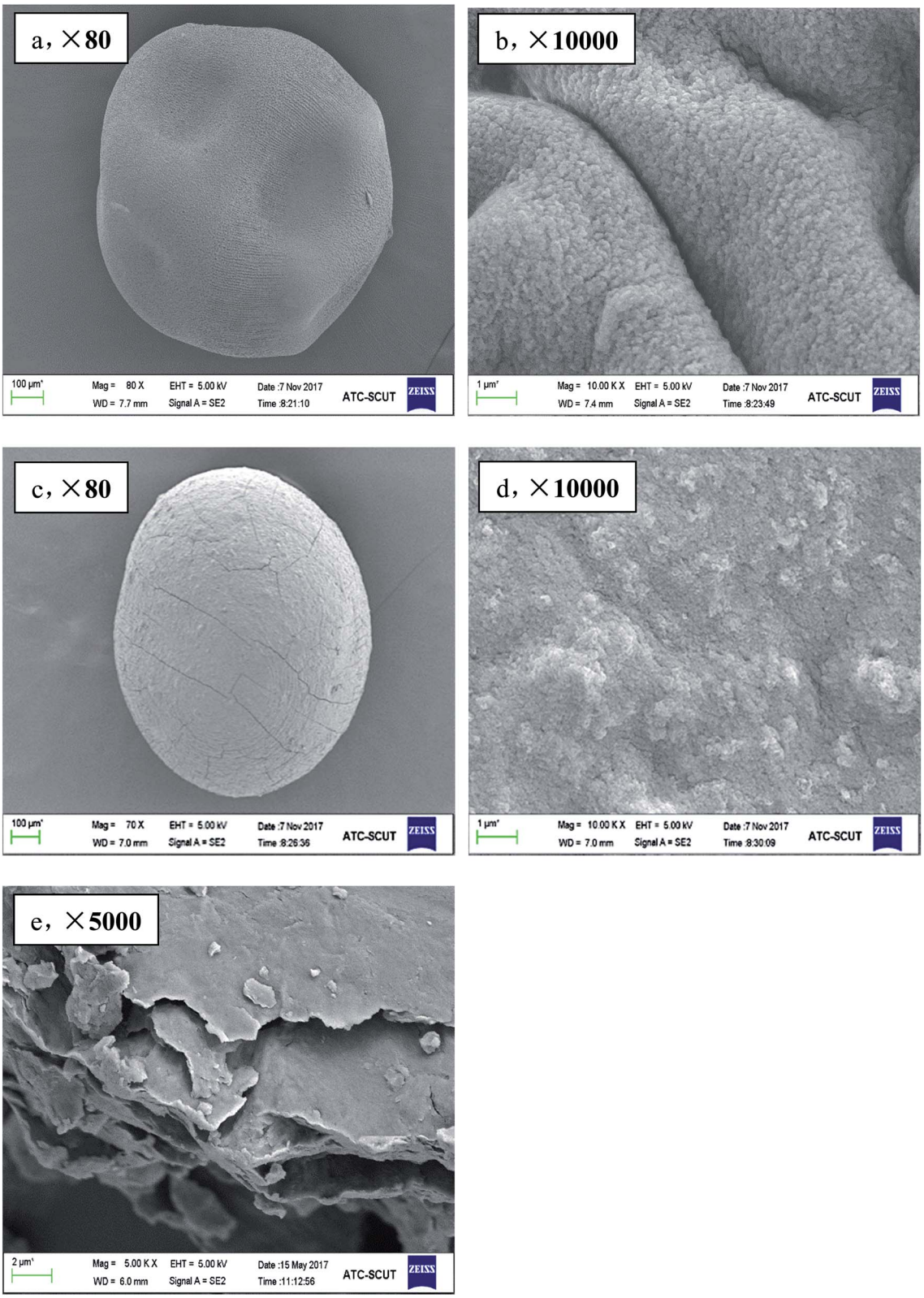

Fig. 2 SEM images of the CMC beads (a and b), CMC–LDH beads (c and d) and LDHs (e).

beads were immersed in $NaNO_3$ solution at room temperature with a constant stirring rate of 180 rpm. Then the beads were rinsed with deionized water several times and dried. After that, the obtained beads were used to adsorb Cr(VI) from aqueous solution. The initial concentration of Cr(VI) and the contact time were 50 mg L^{-1} and 180 min, respectively.

3. Results and discussion

3.1 Characterization of CMC–LDH beads

In order to provide a visual illustration of the removal efficiency of Cr(VI) using the CMC–LDH beads, digital photographs of the different samples were taken, as shown in Fig. 1. All of the beads were spherical in shape, with a diameter of about 0.5–0.8 mm. The color of the Cr(VI) solution became light after treatment with the CMC–LDH beads. However, there was no distinct color loss in the Cr(VI) solution after adsorption by the CMC beads, which is consistent with the color difference between the CMC and CMC–LDH beads after adsorbing Cr(VI). It can be concluded that the CMC–LDH beads can remove Cr(VI) effectively. The morphology of the CMC beads, CMC–LDH beads and LDHs was also studied using SEM and the images are displayed in Fig. 2. According to the figures, the LDH samples exhibited a platelet-like morphology. Severe wrinkles were observed on the surface of the CMC bead, which is related to the partial collapse of the polymer network during drying.[13] However, the surface of the CMC–LDH beads is smoother. Fig. 3 shows the EDS mapping images of the CMC–LDH beads. It is noted that the LDH particles were dispersed in the CMC matrix.

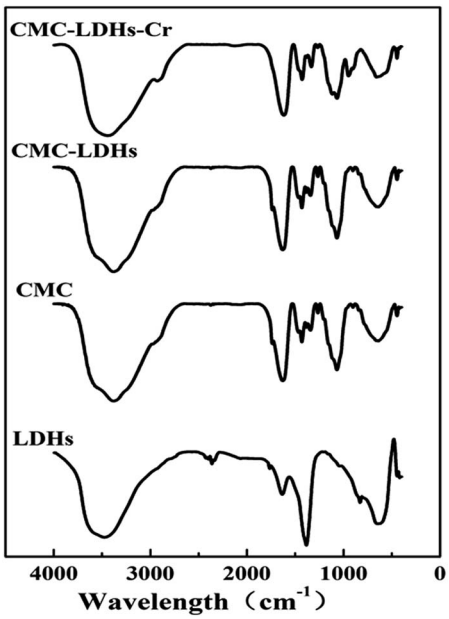

Fig. 4 FTIR spectra of the samples.

Fig. 4 shows the FTIR spectra of the different samples. The broad bands ranging from 3600 to 3400 cm^{-1} are ascribed to the

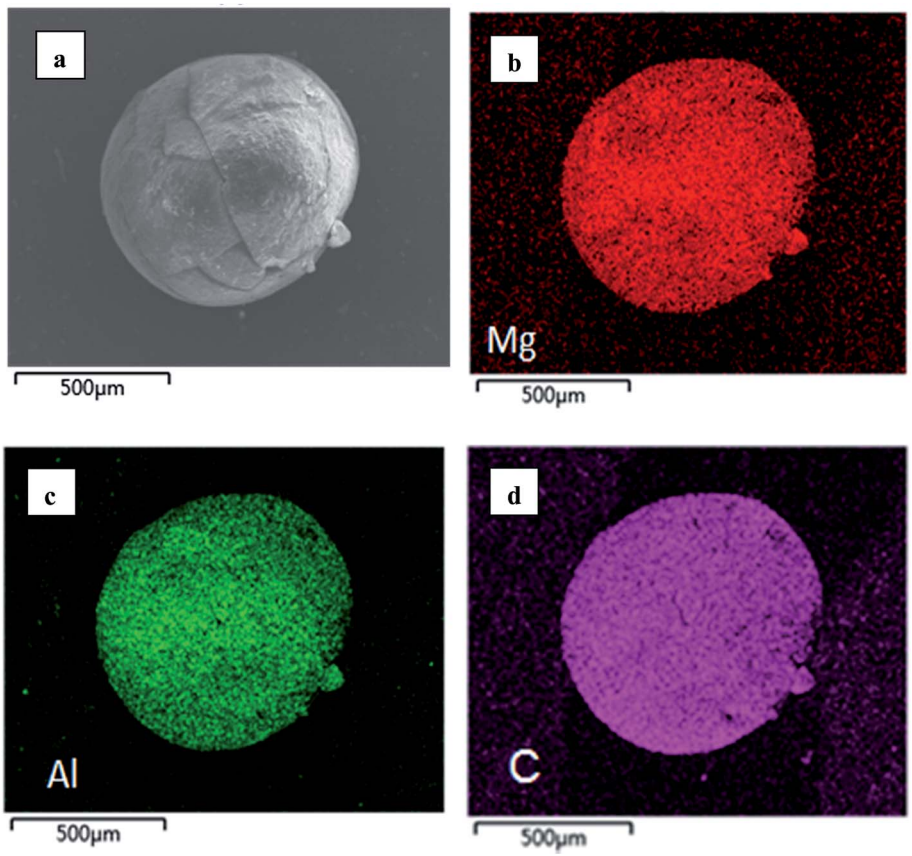

Fig. 3 EDS mapping images of the CMC–LDH beads.

stretching vibrations of the –OH groups. The peaks for CMC and the CMC–LDH beads at 1433 cm^{-1} and 1620 cm^{-1} are attributed to the symmetrical and asymmetrical stretching vibrations of the carboxylate group. The obvious peak for the LDHs at 1380 cm^{-1} is due to the NO_3^- stretching vibration. A new vibration peak at 910 cm^{-1}, for the CMC–LDH beads after adsorption, was observed, revealing the presence of CrO_2^{4-}.

It has been demonstrated from the TG and DTG curves of the CMC–LDH beads (Fig. 5) that there are two main weight loss steps. The first weight loss step below 240 °C is mainly ascribed to water desorption from the CMC–LDH beads, including water loss from CMC and interlayer water loss from the LDHs. It has been reported that all of the interlayer H_2O molecules are removed upon heating to 250 °C,[15] which is mainly related to the distinct peak in the DTG curve at around 230 °C. The second weight loss step occurred within a temperature range of 240 °C to 600 °C, and this is attributed to the decomposition of CMC and the LDHs. The rate of weight loss of the CMC–LDH beads was 52.7% at 600 °C.

3.2 Effect of adsorbent dosage on Cr(VI) uptake

Fig. 6 shows the effect of adsorbent dosage on the removal of Cr(VI). It was found that the removal rate of Cr(VI) increases gradually with the increase of adsorbent dosage, which is ascribed to the greater surface area of the adsorption material and the availability of the increasing adsorption sites. However, a plateau was observed when the dosage was above 14 mg L^{-1}, which is attributed to the increase of vacant active adsorption sites. In other words, Cr(VI) didn't make full use of all the adsorption sites during the adsorption process.

3.3 Effect of contact time on Cr(VI) uptake

The impact of contact time on the removal of Cr(VI) by CMC–LDH beads was studied and the results are shown in Fig. 7. The removal rate showed a rapid increase within the first 30 min, and this then turned into a modest increase during the following adsorption. During the process of adsorption, the adsorbed Cr(VI) had a tendency to desorb into the solution. The desorption function and adsorption function would reach a dynamic equilibrium eventually. Therefore, the amount of Cr(VI) reached a near constant value when the contact time was over 120 min, suggesting that adsorption saturation had been achieved. In order to ensure that the adsorption process reached the equilibrium state, subsequent experiments were conducted for 180 min.

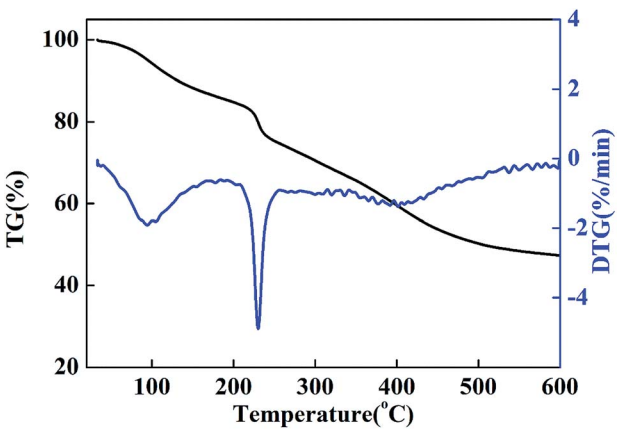

Fig. 5 TG and DTG curves of the CMC–LDH beads.

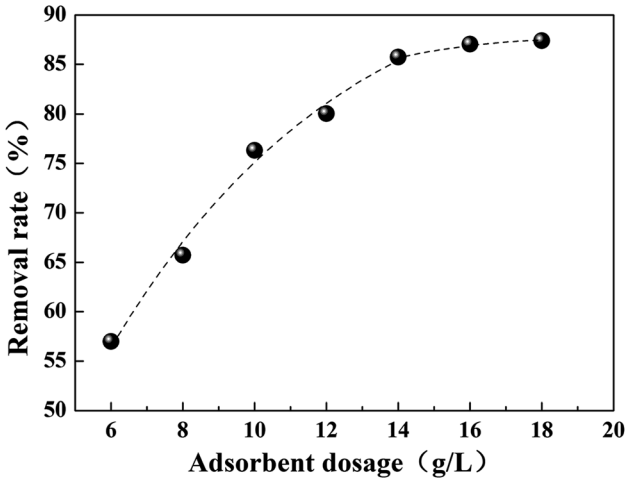

Fig. 6 The effect of adsorbent dosage on Cr(VI) uptake by CMC–LDH beads.

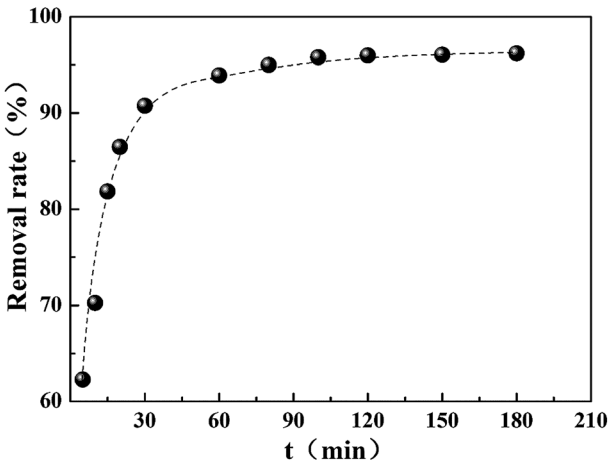

Fig. 7 The effect of contact time on Cr(VI) uptake by CMC–LDH beads.

3.4 Effect of initial pH on Cr(VI) uptake

The effect of the initial pH of the solution on the removal of Cr(VI) was investigated. Fig. 8 shows the adsorption capacity and removal rate at different pH levels. According to the figure, it can be noted that pH had little influence on the adsorption capacity of Cr(VI) by the CMC–LDH beads, and the adsorption capacity showed a reduction from 25.1 mg g^{-1} to 23.2 mg g^{-1} along with the pH increase. The reason for this is because OH^- was adsorbed on the surface of the CMC–LDH beads, resulting in the competitive adsorption of OH^- and Cr(VI) from the solution. Meanwhile, it was observed that the removal rate decreased from 73.6% to 69.9%. The pH values of the Cr(VI)

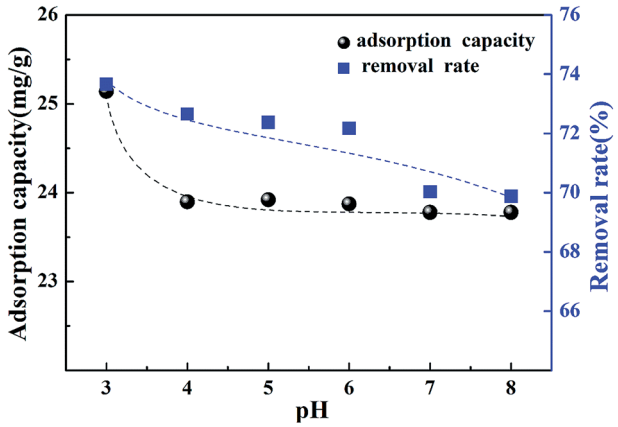

Fig. 8 The effect of pH on Cr(VI) uptake by CMC–LDH beads.

solution before and after adsorption are shown in Table 1. The equilibrium pH of the solution remained steady at 6.3–6.9, which may be related to the adsorption of OH^- in the interlayer position of the LDHs.

3.5 Adsorption kinetics

Mathematical modeling is recognized as a powerful tool for the analysis of the adsorption process. In this paper, both pseudo-first-order and pseudo-second-order kinetic models were applied to investigate the kinetics of Cr(VI) adsorption at various initial concentrations.

Pseudo-first-order model:[16]

$$\ln(q_e - q_t) = \ln q_e - k_1 t \quad (3)$$

Pseudo-second-order model:[17]

$$\frac{t}{q_t} = \frac{1}{k_2 q_e^2} + \frac{t}{q_e} \quad (4)$$

where q_e and q_t are the amounts of Cr(VI) adsorbed (mg g^{-1}) at equilibrium and at any time, respectively. Here t is the adsorption time (min), and k_1 (min^{-1}) and k_2 (g mg^{-1} min^{-1}) are the rate constants for the pseudo-first order and pseudo-second order models, respectively.

On the basis of the equations mentioned above and the laboratory data, the kinetic parameters and the adsorption capacity could be determined using modeling techniques. The kinetic models for Cr(VI) adsorption on the CMC–LDH beads, according to pseudo-first-order and pseudo-second-order kinetics, are shown in Fig. 9. The kinetic constants and correlation coefficients (R^2), obtained using linear regression, for the two models are listed in Table 2. The R^2 value obtained

Table 1 The pH of the Cr(VI) solution before adsorption and after adsorption

Initial pH	3.0	4.0	5.0	6.0	7.0	8.0
Equilibrium pH	6.3	6.4	6.4	6.6	6.8	6.9

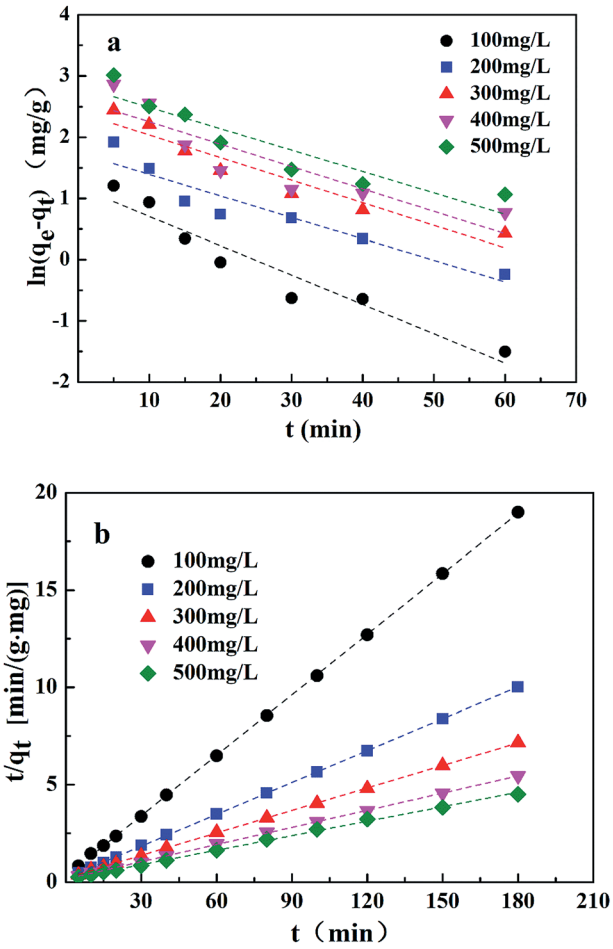

Fig. 9 Adsorption kinetics for Cr(VI) uptake on CMC–LDH beads ((a) pseudo-first-order model; (b) pseudo-second-order model).

from the pseudo-first-order model was lower than that obtained from the pseudo-second-order model, and the calculated q_e obtained from the pseudo-second-order model was much closer to the experimental value of q_e, around 0.999, which confirms that the pseudo-second-order model matches better with the real adsorption process of Cr(VI), in the present research, when compared with the other model. With the increase in the initial concentration of Cr(VI), k_2 gradually became smaller. The higher initial concentration meant that there was a greater probability of the Cr(VI) ions colliding with each other, while the time they took to combine with the active site of the adsorption beads increased, which is consistent with the literature.[18]

3.6 Adsorption isotherms

Langmuir and Freundlich adsorption isotherms are significant for describing the interaction between the adsorbent and adsorbate. The equations are shown as follows:

Langmuir:[19]

$$\frac{C_e}{q_e} = \frac{1}{q_m b} + \frac{C_e}{q_m} \quad (5)$$

Table 2 The pseudo-first-order and pseudo-second-order rate parameters for Cr(VI) adsorption on CMC–LDH beads

	100 mg L^{-1}	200 mg L^{-1}	300 mg L^{-1}	400 mg L^{-1}	500 mg L^{-1}
Pseudo-first-order model					
k_1 (min^{-1})	0.0479	0.0351	0.0369	0.0366	0.035
q_e (mg g^{-1})	3.3	5.7	11.1	13.7	17.1
R^2	0.9285	0.8987	0.9239	0.7956	0.8648
Pseudo-second-order model					
k_2 [g mg^{-1} min^{-1}]	0.0359	0.0154	0.0074	0.0056	0.0046
q_e (mg g^{-1})	9.7	18.3	25.9	34.0	40.2
R^2	0.9999	0.9999	0.9999	0.9997	0.9985
Experimental					
q_e (mg g^{-1})	9.5	18.0	25.1	33.0	39.9

Freundlich:[20]

$$\lg q_e = \frac{1}{n} C_e + \lg K_F \quad (6)$$

where C_e represents the equilibrium ion concentration in solution, q_e is the amount of Cr(VI) adsorbed (mg g^{-1}) in the equilibrium state and q_m (mg g^{-1}) is the maximum uptake of Cr(VI). In addition, b (L mg^{-1}) is a constant that is related to the energy of adsorption in the Langmuir adsorption isotherm, K_F is a constant that represents the adsorption capacity in the Freundlich adsorption isotherm and is related to the bond strength and $\frac{1}{n}$ is a constant corresponding to the adsorption intensity.

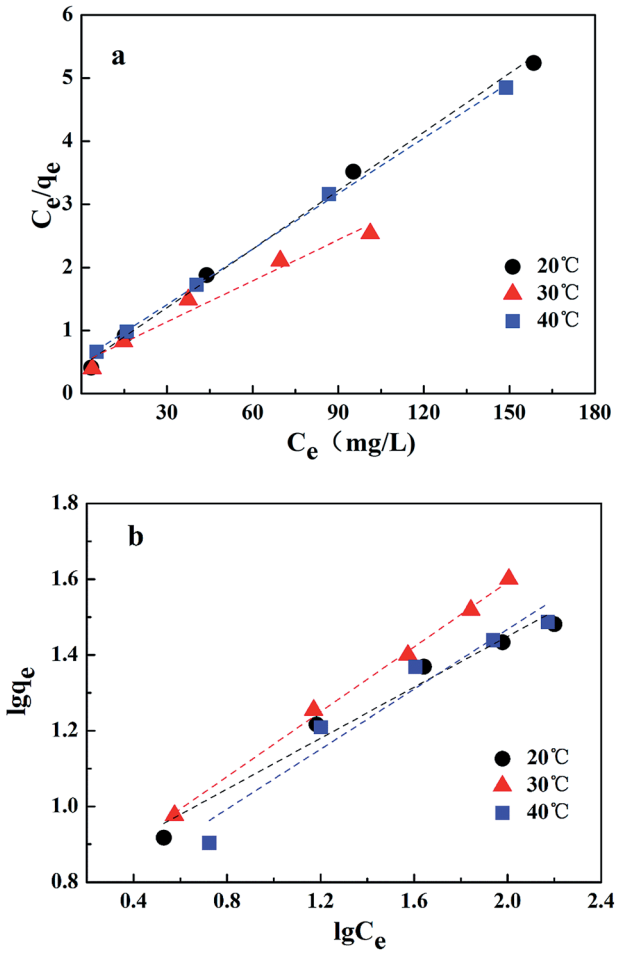

Fig. 10 Adsorption isotherms for Cr(VI) uptake by CMC–LDH beads ((a) Langmuir; (b) Freundlich).

The Langmuir and Freundlich adsorption isotherm models were investigated, as shown in Fig. 10. The experimental data fitted well with these two kinetic models, and the estimated parameters are displayed in Table 3. According to the results obtained using linear regression for the two models, the correlation coefficients (R^2) for both the Langmuir model and the Freundlich model could reach 0.99. It has been revealed in the present research that both these models are reliable for describing the adsorption behavior. The Langmuir isotherm model is based on the assumption that the adsorption sites are identical and energetically equivalent, and only monolayer adsorption occurs in the process.[21] However, the Freundlich isotherm model is based on the assumption of exponentially decaying adsorption site energy distribution and is used for heterogeneous surface energy systems.[22] Therefore, both monolayer and multilayer adsorption were involved in the removal process of Cr(VI) by CMC–LDH beads.

3.7 Desorption and reusability

Recyclability is an important factor to be considered when assessing an adsorbent. The reusability of the CMC–LDH beads

Table 3 Isotherm parameters for Cr(VI) adsorption by CMC–LDH beads

	20 °C	30 °C	40 °C
Langmuir			
b (L mg^{-1})	0.0703	0.0444	0.0549
q_m (mg g^{-1})	32.4	46.1	34.1
R^2	0.9966	0.9680	0.9992
Freundlich			
K_F [mg g^{-1} (L mg^{-1})$^{1/n}$]	0.20	0.16	0.17
$1/n$	0.336	0.4283	0.3957
R^2	0.9704	0.9979	0.9440

Table 4 The reusability behavior of the CMC–LDH beads for Cr(VI) removal

Cycle time	1	2	3	4	5	6	7	8	9	10
Removal rate (%)	94.5	93.9	93.8	92.6	91.9	91.5	90.7	90.1	90.1	89.6

was investigated preliminarily. The removal rate of Cr(VI) by the CMC–LDH beads after different recycling times of desorption was investigated. According to Table 4, the removal rate showed a decline from 94.5% to 89.6% after 10 cycles, which indicates that the CMC–LDH beads are suitable for practical applications.

4. Conclusions

CMC–LDH beads were prepared, characterized and applied for the removal of heavy metal ions in this study. The results confirmed that CMC–LDH beads could remove Cr(VI) from aqueous solution efficiently. It was verified that the pseudo-second-order model was more appropriate for the actual adsorption process of Cr(VI), in the present research, which was in accordance with the adsorption kinetics. The adsorption mechanisms, which included both a monolayer and multilayer adsorption process, were investigated using adsorption isotherms. The CMC–LDH beads could be reused and the removal rate was 89.6% after 10 cycles. Overall, CMC–LDH beads could be recognized as a promising adsorbent for Cr(VI) uptake on account of their high removal rate, excellent reusability and environmental friendliness.

Conflicts of interest

There are no conflicts to declare.

Acknowledgements

The authors acknowledge the National Key R&D Program of China (2017YFB0308003), the Science and Technology Planning Project of Guangdong Province (2015A020215007), the Natural Science Foundation of China (No. 31670586), the Fundamental Research Funds for the Central Universities (2017ZD091 and 2017MS073), and the State Key Laboratory of Pulp and Paper Engineering Program (2016C05) for sponsoring this research.

References

1 M. D. Cohen, B. Kargacin, C. B. Klein, *et al.*, Mechanisms of Chromium Carcinogenicity and Toxicity, *Crit. Rev. Toxicol.*, 1993, **23**(3), 255–281.
2 J. E. Mclean, L. S. Mcneill, M. Edwards, *et al.*, Hexavalent chromium review: Part 1, health effects, regulations, and analysis, *J. Am. Water Works Assoc.*, 2012, **104**(6), 348–358.
3 M. Chebeir and H. Liu, Kinetics and Mechanisms of Cr(VI) Formation *via* the Oxidation of Cr(III) Solid Phases by Chlorine in Drinking Water, *Environ. Sci. Technol.*, 2016, **50**(2), 701–710.
4 F. Fu and Q. Wang, Removal of heavy metal ions from wastewaters: a review, *J. Environ. Manage.*, 2011, **92**(3), 407–418.
5 M. J. Waring and D. Parsons, Physico-chemical characterisation of carboxymethylated spun cellulose fibres, *Biomaterials*, 2001, **22**(9), 903–912.
6 M. Boruah, P. Gogoi, *et al.*, Biocompatible carboxymethyl-cellulose-*g*-poly(acrylic acid)/OMMT nanocomposite hydrogel for *in vitro* release of vitamin B12, *RSC Adv.*, 2014, **4**(83), 43865–43873.
7 C. Xing, F. Musharavati, H. Li, *et al.*, Synthesis, characterization, and properties of nickel–cobalt layered double hydroxide nanostructures, *RSC Adv.*, 2017, **7**(62), 38945–38950.
8 J. He, M. Wei and B. Li, *et al.*, *Preparation of Layered Double Hydroxides*, Springer, Berlin, Heidelberg, 2006, pp. 345–373.
9 G. Mishra, B. Dash and S. Pandey, Layered double hydroxides: A brief review from fundamentals to application as evolving biomaterials, *Appl. Clay Sci.*, 2018, **153**, 172–186.
10 Y. H. Chuang, M. T. Yu, M. K. Wang, *et al.*, Removal of 2-Chlorophenol from Aqueous Solution by Mg/Al Layered Double Hydroxide (LDH) and Modified LDH, *Ind. Eng. Chem. Res.*, 2008, **47**(11), 3813–3819.
11 T. Zhang, Q. Li, H. Xiao, *et al.*, Synthesis of Li–Al Layered Double Hydroxides (LDHs) for Efficient Fluoride Removal, *Ind. Eng. Chem. Res.*, 2012, **51**(35), 11490–11498.
12 M. Yadollahi, H. Namazi and M. Aghazadeh, Antibacterial carboxymethyl cellulose/Ag nanocomposite hydrogels cross-linked with layered double hydroxides, *Int. J. Biol. Macromol.*, 2015, **79**, 269–277.
13 S. Barkhordari and M. Yadollahi, Carboxymethyl cellulose capsulated layered double hydroxides/drug nanohybrids for Cephalexin oral delivery, *Appl. Clay Sci.*, 2016, **121–122**, 77–85.
14 T. Toraishi, S. Nagasaki and S. Tanaka, Adsorption behavior of IO_3^- by CO_3^{2-}- and NO_3^--hydrotalcite, *Appl. Clay Sci.*, 2002, **22**(1), 17–23.
15 G. S. Thomas, A. V. Radha, P. Vishnu Kamath, *et al.*, Thermally Induced Polytype Transformations among the Layered Double Hydroxides (LDHs) of Mg and Zn with Al, *J. Phys. Chem. B*, 2006, **110**(25), 12365–12371.
16 A. R. Ricardo, G. Carvalho, S. Velizarov, *et al.*, Kinetics of nitrate and perchlorate removal and biofilm stratification in an ion exchange membrane bioreactor, *Water Res.*, 2012, **46**(14), 4556–4568.
17 M. Hamayun, T. Mahmood, A. Naeem, *et al.*, Equilibrium and kinetics studies of arsenate adsorption by $FePO_4$, *Chemosphere*, 2014, **99**(3), 207–215.
18 S. Chen, Q. Yue, B. Gao, *et al.*, Removal of Cr(VI) from aqueous solution using modified corn stalks:

Characteristic, equilibrium, kinetic and thermodynamic study, *Chem. Eng. J.*, 2011, **168**(2), 909–917.

19 P. Baskaralingam, M. Pulikesi, D. Elango, *et al.*, Adsorption of acid dye onto organobentonite, *J. Hazard. Mater.*, 2006, **128**(2–3), 138–144.

20 M. Dalaran, S. Emik, G. Güçlü, *et al.*, Removal of acidic dye from aqueous solutions using poly(DMAEMA–AMPS–HEMA) terpolymer/MMT nanocomposite hydrogels, *Polym. Bull.*, 2009, **63**(2), 159–171.

21 I. Langmuir, The adsorption of gases on plane surfaces of glass, mica and platinum, *J. Chem. Phys.*, 1918, **40**(12), 1361–1403.

22 H. Freundlich, Of the adsorption of gases. Section II. Kinetics and energetics of gas adsorption. Introductory paper to Section II, *Trans. Faraday Soc.*, 1932, **28**(7), 195–201.